

# Applications of an Expanded ZDR Scale

Valery Melnikov<sup>\*</sup>, Richard Murnan<sup>+</sup>, and Donald Burgess<sup>\*</sup>

<sup>\*</sup> CIMMS, University of Oklahoma and National Severe Storms Laboratory, Norman, OK.

<sup>+</sup> NWS, Radar Operations Center, Norman, OK.

## 1. Introduction

The WSR-88D radar network is currently running RDA/RPG Build 18. Differential reflectivity in this build (and in earlier ones) is measured in an interval of -7.9 to 7.9 dB. This interval follows from 1 byte representation of a ZDR value. The total measurement ZDR span is 15.8 dB, therefore, the accuracy of representation is  $15.8/256 = 0.062$  dB (256 is the number of steps in a representation of a value with a 1 byte code).

It has been noticed that +7.9 dB maximum ZDR value is not sufficient to observe weather systems containing snow or ice crystals. To cover the maximal ZDR values from such objects, the measurement ZDR interval should be enlarged. An expanded ZDR interval is also needed for correct ZDR measurements of atmospheric biota. ZDR values from birds and insects frequently exceed 7.9 dB. To better distinguish echoes from birds and insects, a larger measurement ZDR interval is needed.

ZDR values in light-to-moderate rain and snowfalls are frequently less than 1 dB. To use ZDR values for quantitative precipitation estimates (QPE) in such precipitation, ZDR should be measured with an accuracy of 0.1 dB. This accuracy has been indicated in the WSR-88D specifications and is an ultimate goal of ZDR measurements. To achieve a 0.1 dB accuracy of ZDR measurements, the precision of measured values should be at least half of this accuracy, i.e., 0.05 dB. The current precision is 0.062 dB and, therefore, it is desirable to be improved.

The needs to enlarge the measurement ZDR span and to decrease the representation of the values make it desirable to change the current 1-byte representation with a larger one. Build 19 will feature a larger ZDR span from -10 to +20 dB and an accuracy of ZDR representation less than 0.05 dB.

In this report,

- Radar data showing limitations of the current ZDR interval ( $\pm 7.9$  dB) are presented in section 2.
- ZDR values from various types of radar echoes are discussed in section 3 to obtain a desirable ZDR span.

- Radar observations with WSR-88D KOUN running an experimental Build 19 are shown in section 4.
- A summary of results and conclusions are in section 5.

## **2. WSR-88D ZDR span on the RDA/RPG Builds prior to Build-19**

Current RDA/RPG Build 18 has the measurement ZDR interval from -7.9 to +7.9 dB. This interval has been chosen by the manufacturer of the WSR-88D's dual-polarization upgrade and covers the most frequent values of ZDR from clouds and precipitation. However, the extreme ZDR values from ice clouds are out of this span (section 3) and to cover all possible ZDR values, the measurement ZDR interval should be enlarged. An interval of  $\pm 7.9$  dB resulted from a representation of the ZDR variable with one byte. The base WSR-88D's variables (Z, V, and W) are coded with one byte format, which is sufficient to deliver the variables with needed accuracy. Two parameters characterize representation of the radar variables in the WSR-88D: accuracy and precision. The accuracy is a parameter showing needed measurement accuracy. The precision shows the minimal quantization step for the variable. To measure a value with a given accuracy, the precision should be at least half of the accuracy. For instance, the accuracy of velocity measurements is specified at 1 m/s and the precision is 0.5 m/s. For reflectivity, the accuracy and precision are 1 dBZ and 0.5 dB, respectively. These requirements can be fulfilled with a representation of the base variables with one byte, i.e., with quantization by 256 steps.

For WSR-88D radars, the accuracy of ZDR measurements has been specified at 0.1 dB, which is an ultimate goal of these measurements. This accuracy has been specified for measurements in light rain and snow, where ZDR values mostly are lower than 1 dB and to use them quantitatively, an accuracy of 0.1 dB is desirable. To take measurements with this accuracy, precision of measurements should be at least twice as smaller, i.e., 0.05 dB. For a one-byte representation, this precision would cover an interval of  $\pm 6.4$  dB (the whole interval is 12.8 dB and the number of steps is 256, then the precision is  $12.8/256 = 0.05$  dB). This would be a too short ZDR measurement interval, because it was known at that time that the maximal ZDR from ice clouds can exceed 7 dB (e.g., Gossard and Strauch 1983). The WSR-88D manufacturer has enlarged the measurement ZDR interval to  $\pm 7.9$  dB that made the precision of one-byte representation of 0.06 dB ( $2 \cdot 7.9/256 = 0.06$ ). This measurement interval covers the most frequent ZDR values from clouds and precipitation.

Radar observations with WSR-88Ds have shown that the  $\pm 7.9$  dB ZDR interval does not cover all possible values from weather objects. An example of high ZDR is presented in Fig. 1. One can see that the southeast part of radar echo has ZDR values higher than 6 dB, which is the last color in the ZDR scale. Fig. 2 presents a distribution of ZDR values from the lowest sweep shown in Fig. 1. A strong spike in the distribution can be seen at the very right end of the distribution. This spike is a result of the limited ZDR interval. All ZDR values greater than 7.9

dB are truncated by the processor to 7.9 dB, and that makes the spike in the distribution in Fig. 2. For a correct representation of ZDR values, a larger ZDR interval is needed.

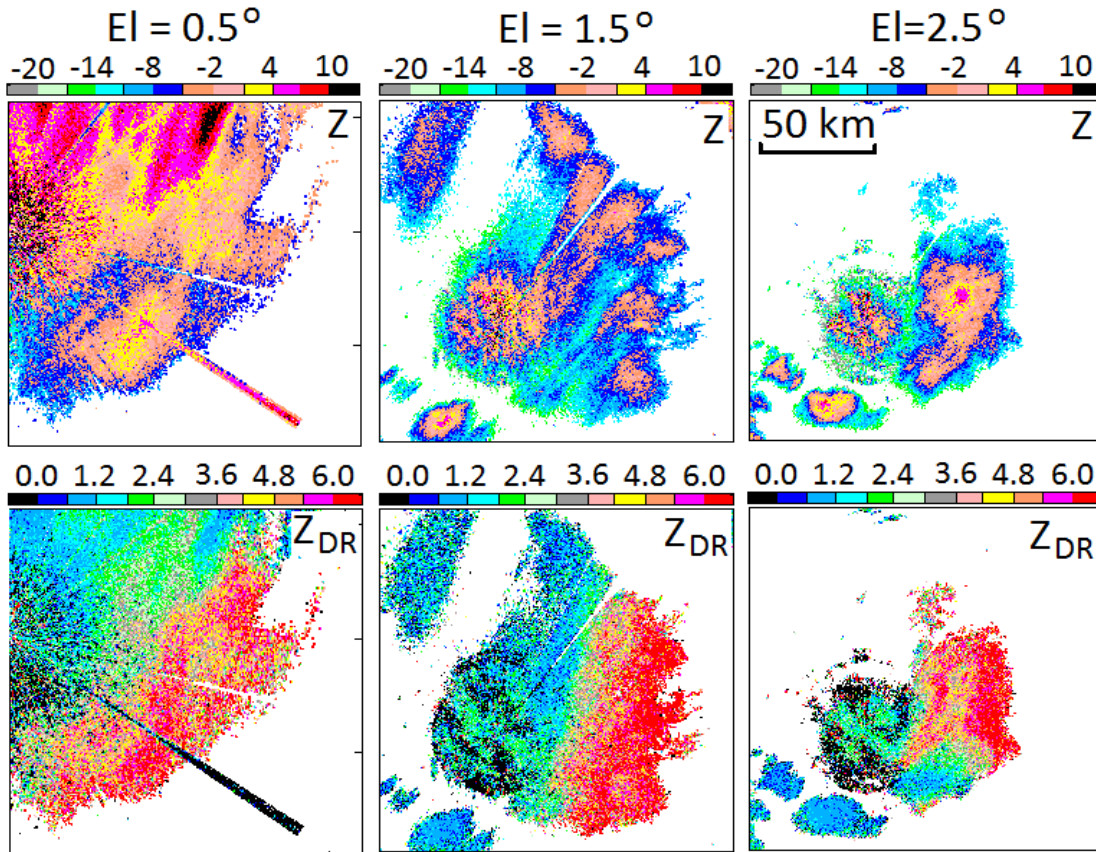


Fig. 1. Fields of reflectivity (the top row) and ZDR (bottom row) at antenna elevations of 0.5, 1.5, and 2.5°. WSR-88D KOUN 1 Feb 2011 at 1948 UTC.

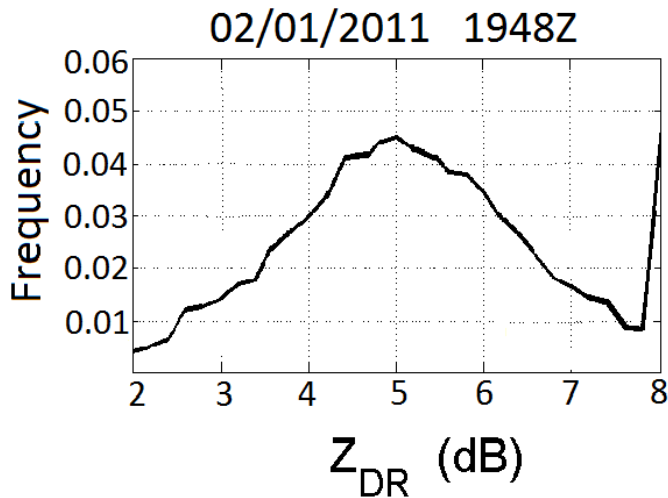


Fig. 2. Distribution of ZDR values from the 0.5° elevation shown in Fig. 1.

The limited ZDR interval has a strong impact on values from atmospheric biota. WSR-88Ds are capable of observing birds, bats, and insects in the atmosphere. Those species produce reflectivity values similar to ones from light precipitation and caused problems in distinguishing weather and biota objects in the non-polarimetric WSR-88Ds. Light precipitation can be seen in Fig. 3 to the far west from the radar, beyond the west Oklahoma border. The data were collected with WSR-88D KTLX (Oklahoma City, OK) running Build 18. Reflectivity from that precipitation is about the same as one from biota closer to the radar. The ZDR values from the precipitation and biota (Fig. 4) are different: ZDR from precipitation is about 0 dB, whereas ZDR from biota are of the very high values. The ZDR variable is one of the dual-polarization parameters used to distinguish weather from biota echoes: higher ZDR values and lower correlation coefficients allow for the separation of echoes from weather and biota.

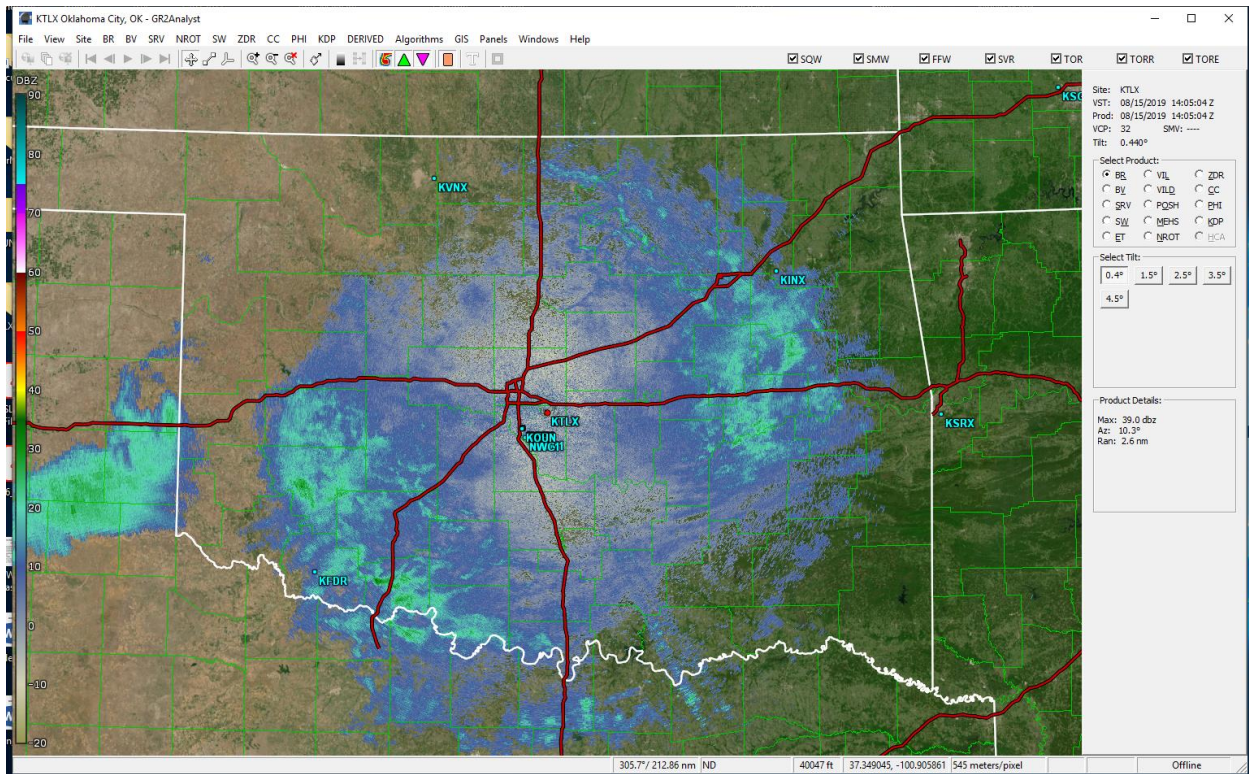


Fig. 3. Reflectivity field from KTLX on 15 Aug. 2019 at 1405 UTC at an elevation of 0.5°.

A histogram of ZDR values from the case in Fig. 4 is shown in Fig. 5. It can be seen a strong spike in the distribution at ZDR = 8 dB. This is a result of clipping large ZDR values to 7.9 dB. This distribution shows a strong limitation of the current ZDR interval in observations of atmospheric biota. It is desirable to enlarge the ZDR interval to better distinguish insects and birds in the air. This would be useful for many applications. For instance, birds are a hazard for aviation. Flying birds strongly impact the obtaining of atmospheric winds from radar data. If bird

echoes can be eliminated from observations, then the wind can be obtained with higher confidence.

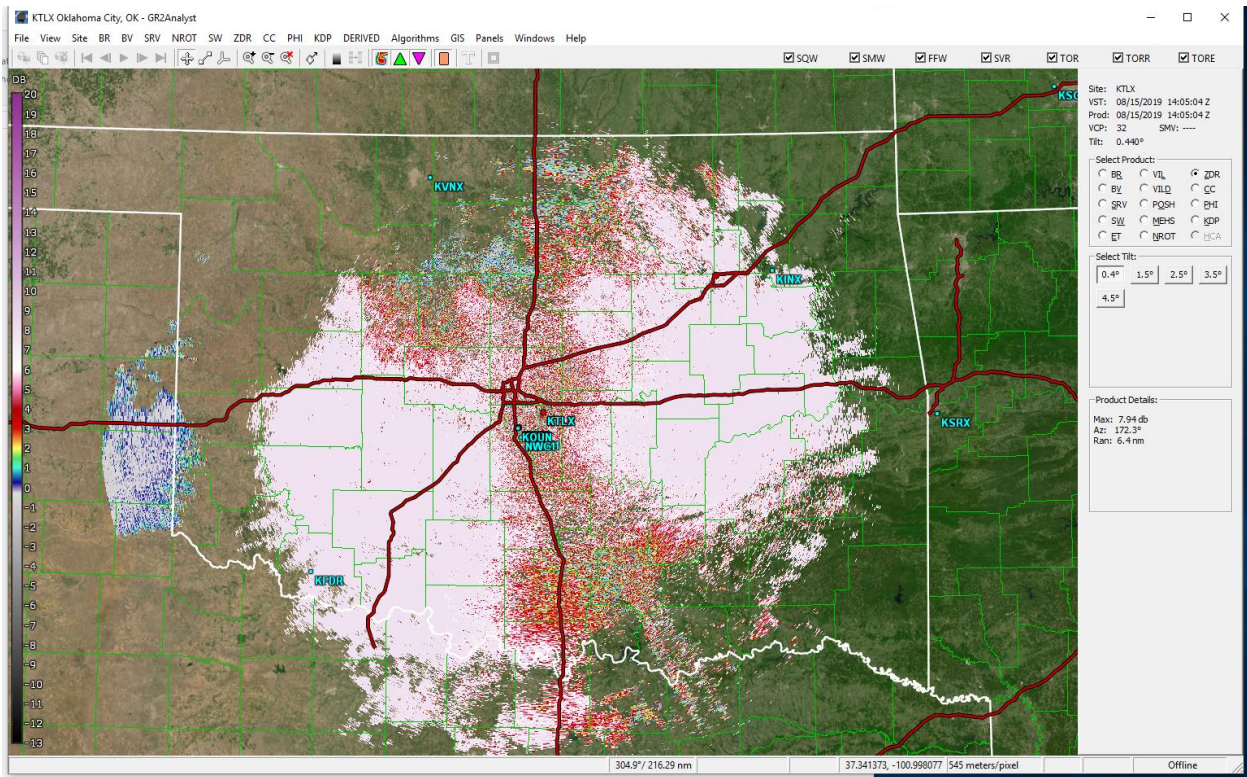


Fig. 4. As in Fig. 3, but for ZDR.

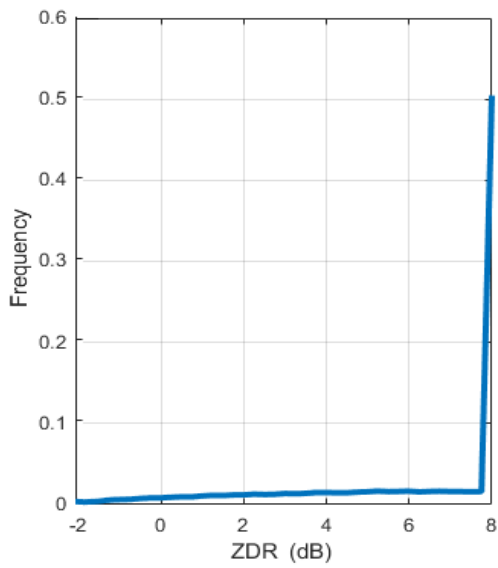


Fig. 5. Histograms of ZDR values for the case in Fig. 4. From Build 18 level-2 data.

### 3. ZDR values from various targets

This section contains data collected from different targets observed with WSR-88Ds to establish boundaries of ZDR values and to justify the requirements for a measurement ZDR interval. To obtain the boundaries of ZDR values from various targets, data of unbound ZDR measurements are needed. Such data cannot be obtained from the current WSR-88D's ZDR values because they are clipped at  $\pm 7.9$  dB. The true ZDR can be obtained from the level-1 data, i.e., from I-Q radar signals that can be obtained from the RDA, not from the RPG. Below, ZDR values obtained from level-1 data are presented and compared, in some cases, with those from ZDR RPG values. The level-1 data are limited at present, so the presented ZDR values could not represent all possible values, but they show the "first order" width of a needed ZDR span. For weather objects, however, the ZDR span must cover all possible values.

#### 3.1. Clouds and precipitation

For dual-polarization radar employing alternate polarization, the maximal possible ZDR is 10 dB (e.g., Gossard and Strauch 1983). This value can be observed in clouds and thunderstorms from thin ice plate-like particles. A sketch of a particle is shown in Fig. 6a, where the angle  $\theta$  is the canting angle and the angle  $\varphi$  is the orientation angle relative to the radar beam. In thunderstorms, ice particles can be aligned by strong in-cloud electric fields so that the angles  $\theta$  and  $\varphi$  can be any in intervals  $0-180^\circ$  and  $0-360^\circ$ , respectively. ZDR from ice particles also depends on the differential phase ( $\psi_i$ ) between horizontally and vertically polarized waves incident on the particle. The ZDR values from thin ice plates depends upon three parameters:  $\theta$ ,  $\varphi$ , and  $\psi_i$ . (RPI MOU-2019 report). The absolute maximal ZDR is plotted in Fig. 6b as a function of the phase  $\psi_i$ . One can see that the maximum ZDR values can reach 12.3 dB. The latter value is attained at  $\psi_i = 0$  and  $180^\circ$ . So the upper limit of ZDR interval for WSR-88Ds must be at least 12.3 dB for observations of hydrometeors.

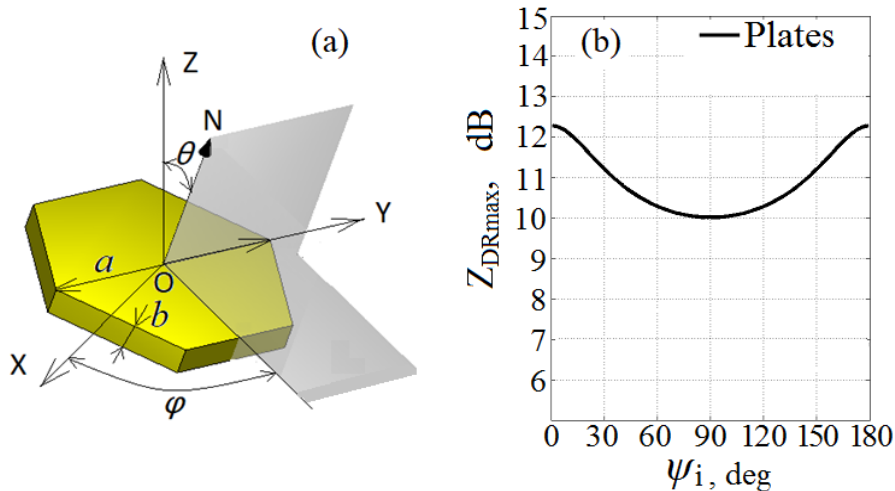


Fig. 6. (a): Hexagonal ice plate with dimensions  $a$  and  $b$  oriented at angles  $\theta$  and  $\varphi$  relative to radar beam. The axis OX is directed toward radar. The axis OZ is vertical. (b): Maximum ZDR values from thin ice plates as a function of the differential phase between the incident horizontally and vertically polarized waves (adopted from RPI MOU-2019 Report, Task 10).

Fig. 7 shows a vertical cross section of clouds observed with KOUN on Dec. 4, 2008. It was a case with overcast nonprecipitating stratiform clouds of reflectivities less than 0 dBZ. Level-1 data were collected on that day that allowed obtaining a ZDR values without limitations of  $\pm 7.9$  dB. It can be seen from Fig. 7 that the cloud echo are contaminated with ground clutter leftovers at distances within 16 km. These contaminations increase at closer distances due to signals coming through the antenna sidelobes.

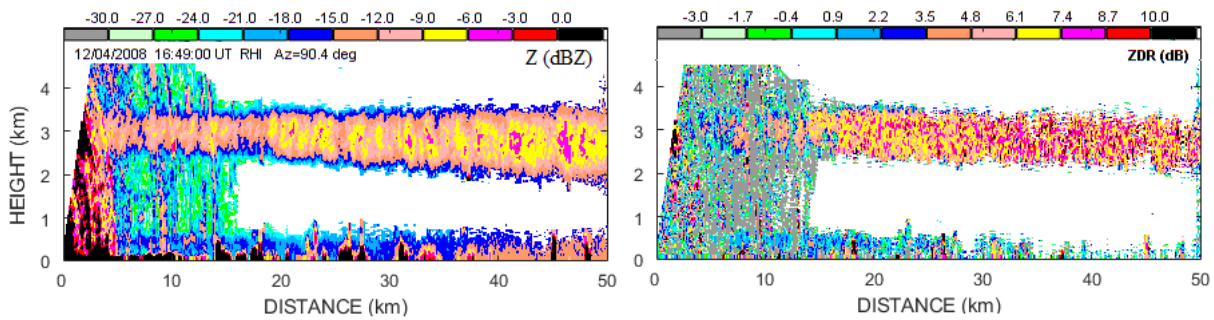


Fig. 7. Vertical cross section collected with KOUN on Dec.4, 2008 at 1649 UTC at an azimuth of  $90.4^\circ$ . The images have been produced from the level-1 data. Ground clutter leftovers can be seen within a distance of 16 km.

A distribution of ZDR values from the case in Fig. 7 is shown in Fig. 8 for distance beyond 16 km to eliminate contaminations from the clutter leftovers. It can be seen that the median ZDR is at about 8 dB and the distribution has a long tail to high values up to 15 dB. These very large ZDR values are a result of two features: a) high intrinsic ZDR values from the particles and b) natural fluctuations of ZDR estimates. It was indicated before that the maximal ZDR from ice particles can be 12.3 dB. This value is the mean one. Radar variables are estimates, because they are obtained from a limited number of radar pulses, i.e., during a limited dwell time. Because of natural fluctuations of radar signals due to reshuffling scatters in the radar resolution volume, the estimates of the intrinsic radar variables are measured. The estimates are also impacted by the values of signal-to-noise ratios, spectrum width, and correlation coefficient. Fig. 8 shows that to account for natural fluctuations of the ZDR estimate, the upper bound of the measurement ZDR interval should be at about 15 dB.

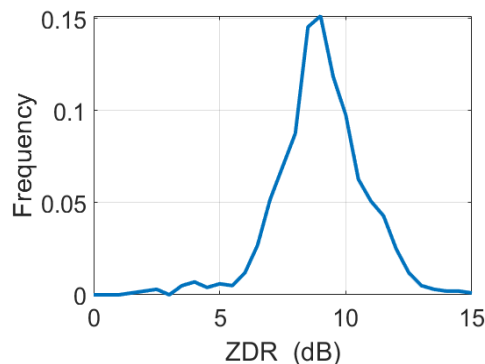


Fig. 8. Distribution of ZDR for the case in Fig. 7 for distances beyond 16 km.

Negative ZDR values are also observed from weather objects. There are three origins of negative ZDR values: a) vertically oriented ice crystals in thunderstorms, b) differential attenuation of signals, and c) resonance scattering from large hailstones. Theoretically, the minimal negative ZDR value from ice crystals is -12.3 dB, i.e., the maximal value, discussed above, but with negative sign. However, such ZDR values have not been observed with the WSR-88Ds. The minimal ZDR values observed with KOUN in thunderstorms were about -4.5 dB. The attenuation impacts on ZDR are discussed in the next subsection.

Large hailstones can be at resonance sizes at S band that makes ZDR values from hail cores negative. ZDR values from hailstones depend on many parameters; the size, wetness, oblateness, and tumbling are among those. Theoretically, the minimum and maximum ZDR values from wet hailstones are about -2 and +5 dB, respectively, for moderate oblateness of about 0.7-0.8. Picca and Ryzhkov (2012) observed minimal and maximal ZDR at -1 to +4.5 dB, respectively, in a hailstorm in Oklahoma on 16 May, 2006.

### **3.2. Attenuation impacts**

Differential attenuation impacts measured ZDR. At S frequency band, changes in ZDR values in rain depend on the changes in differential phase as,  $\Delta ZDR$  (dB) =  $-0.004 \Delta\Phi_{DP}$  (deg). The minus sign indicates a decrease in  $Z_{DR}$  due to attenuation. Radar observations show that  $\Delta\Phi_{DP}$  can reach  $500^\circ$  in heavy precipitation leading to decreases in ZDR as high as 2 dB. So the differential attenuation can lower the intrinsic  $Z_{DR}$  values by as much as -2 dB at S band. In thunderstorms, where ice crystals can be aligned by electric fields,  $\Delta ZDR$  can be positive because vertically oriented ice crystals change the  $\Delta ZDR$  sign because the sign of  $\Delta\Phi_{DP}$  is negative. It is hard to estimate  $\Delta\Phi_{DP}$  in vertically oriented ice crystals because a contribution from the differential phase upon scattering should be accounted for. Radar observations do not show significant positive  $\Delta ZDR$  in thunderstorms. Therefore, the attenuation impacts can be estimated to lie in an interval from 0 to -2 dB.

### **3.3. Dust storms**

Dust storms exhibit ZDR values as high as 12 dB. An example is shown in Fig. 9, where the dust storm can be seen in a form of an ark located close to Phoenix, AZ; the location of Phoenix is shown with a dot in the left panel. Very high ZDR values up to 12 dB were observed, which could be a result of insects and/or debris trapped in the storm's outflow. Fig. 9 has been generated from the level-1 data collected during the Doppler cut with the unambiguous distance of 150 km.

Fig. 10 has been obtained from level-2 data collected at the same time. The dust storm is shown with the black arrow. A ZDR distribution from the storm obtained from level-2 data is shown in Fig. 11. It can be seen that the vast majority of ZDR values are higher than 7.9 dB and create a spike at the end of distribution. This example demonstrates that a larger measurement ZDR interval is needed to correctly represent ZDR values in dust storms.

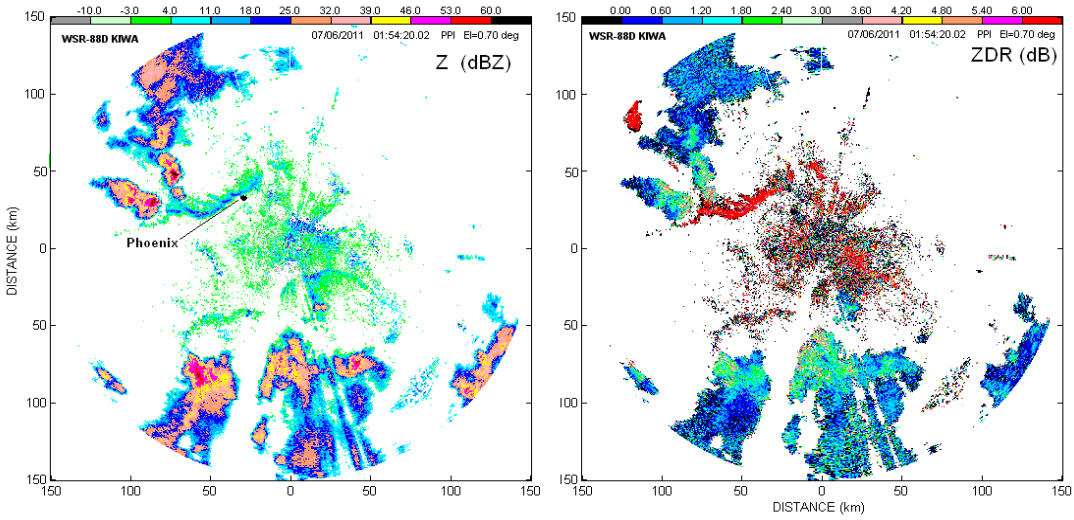


Fig. 9. Reflectivity (left) and ZDR (right) fields from WSR-88D KIWA (Phoenix, AZ) collected on July 6, 2011 at 0154Z at the elevation of 0.5°.

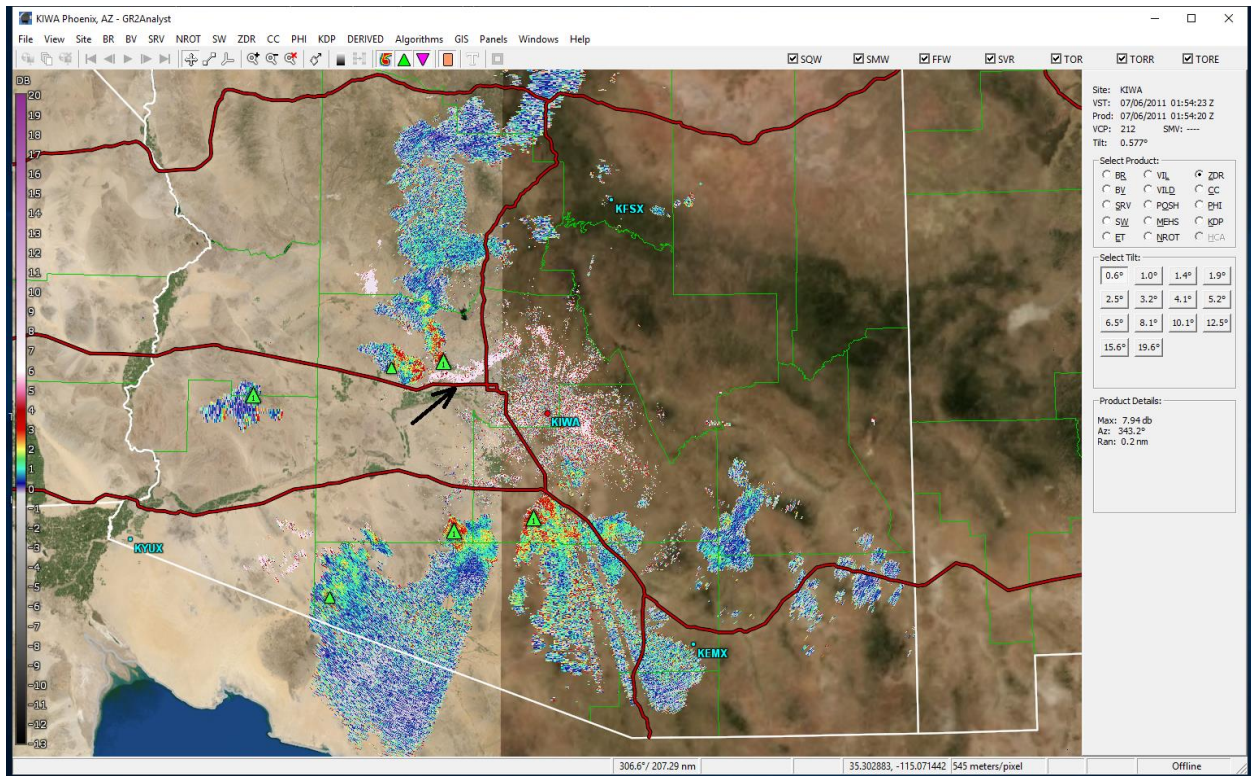


Fig. 10. As in Fig. 9, but for level-2 data.

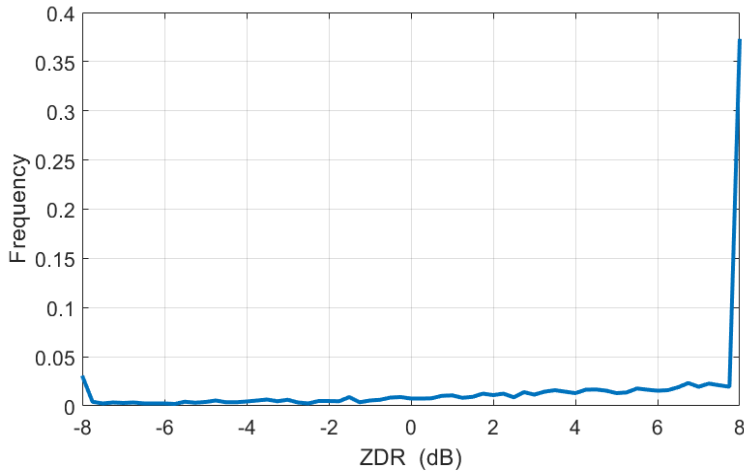


Fig. 11. Histogram of ZDR values from the dust storm obtained from level-2 data in Fig. 10.

### 3.4. Ground clutter

Unsuppressed ground clutter exhibits a very large span of ZDR values. An example of ZDR distribution from the ground is shown in Fig. 12. The level-1 data were collected with KOUN on 30 March, 2018. No ground filter has been applied to the data. To exclude possible contamination from atmospheric biota, signals with SNR > 20 dB have been processed. One can see that  $Z_{DR}$  values span an interval larger than  $\pm 20$  dB. About 95% of data lie in an interval  $\pm 14$  dB. Note that the data were collected in central Oklahoma. In other region, the distribution can be different.

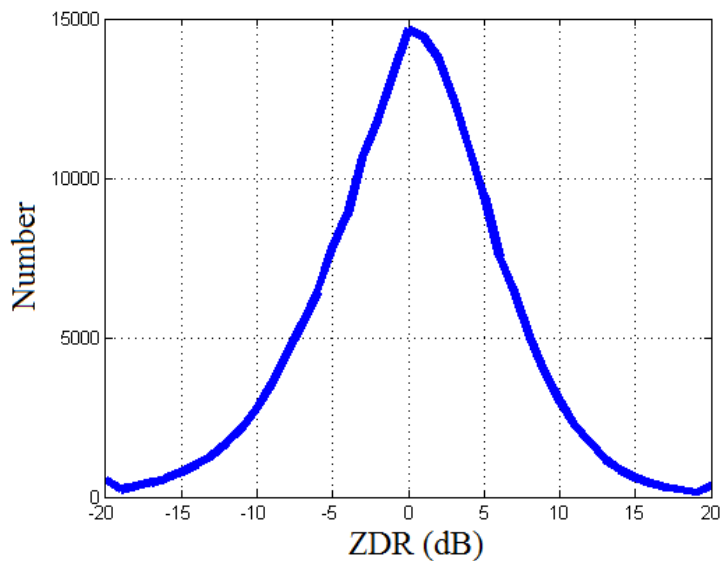


Fig. 12. Distribution of ZDR values from ground clutter. WSR-88D KOUN, 30 March 2018, 1000 – 1200 Z, antenna elevation is  $0.5^\circ$ , in short pulse mode.

### 3.5. Sea clutter

An example of reflectivity field from sea clutter is shown in Fig. 13. The data were collected with the WSR-88D KMHX at Moorhead City, NC on June 23, 2011. Radar data from two areas of sea clutter have been analyzed; these areas are numbered with 1 and 2 in the figure. Area 1 is closest to the radar at a distance to its center of about 115 km from the radar, and the distance to maximal reflections in area 2 is at about 200 km from the radar. Level-1 data were collected at that time, allowing unclipped ZDR values shown in Fig. 14. One can see that the median ZDR is negative and the spread in the values is large. 95% of ZDR data lie in an interval -9 to +6 dB; the maximal and minimal ZDR values are +15 and -15 dB, respectively.

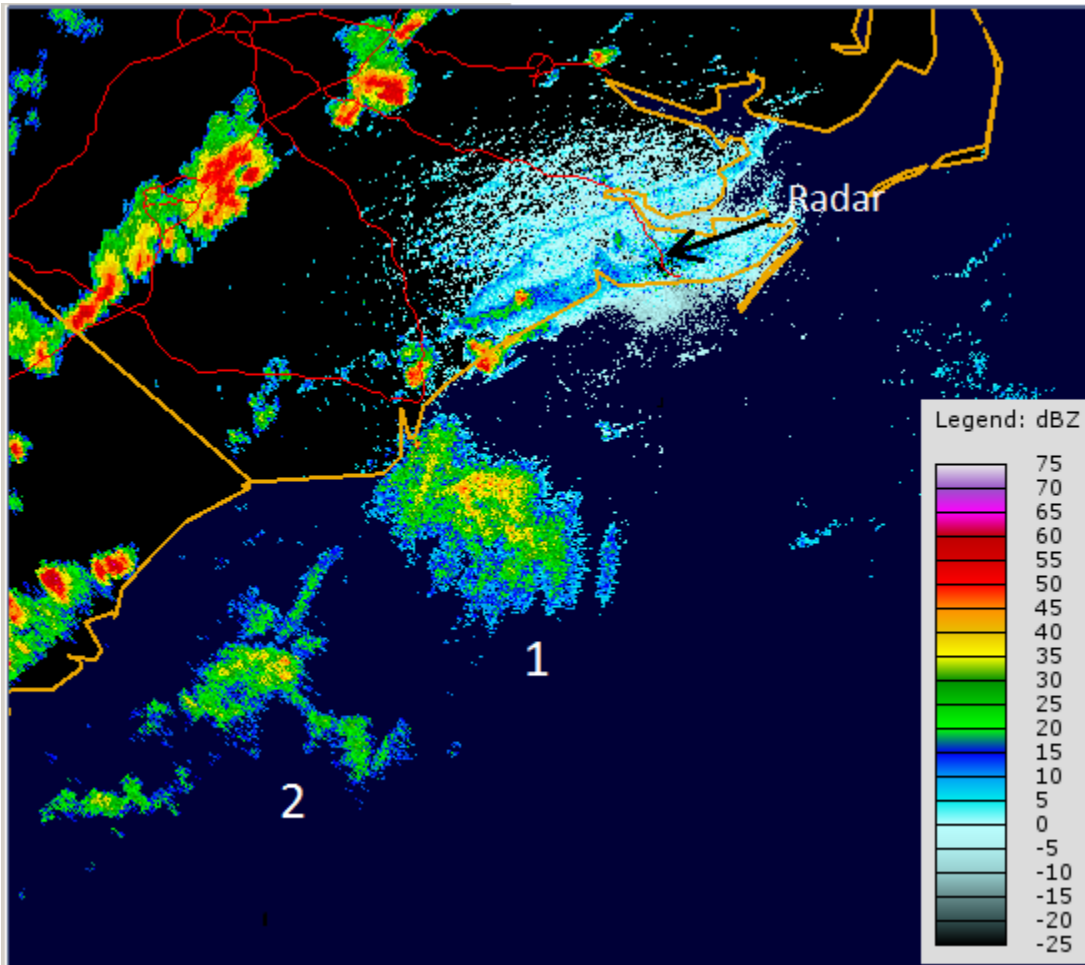


Fig. 13. Two main patches of sea clutter observed with KMHX on June 23, 2011 at 2047Z at an elevation of 0.5°.

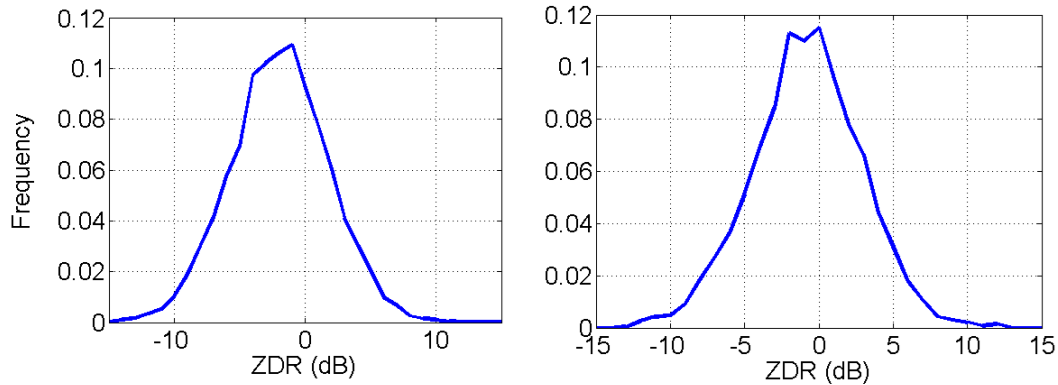


Fig. 13. Distributions of the ZDR values in clutter patch #1 (left panel) and #2 (right panel).

One more example of sea clutter is shown in Fig. 14, collected with KNKX (San Diego, CA) on 16 Aug. 2016. Level-2 data are available for this case. A corresponding ZDR distribution is shown in Fig. 15. A strong spike in ZDR can be seen at +8 dB, i.e., at the maximum value of the measurement ZDR interval. This case shows that ZDR from sea clutter could depend on the wind at sea and orientation of sea waves/tides relative to the radar beam. Cases in Figs. 12 and 14 show that correct ZDR measurements in sea clutter are possible for a larger ZDR interval.

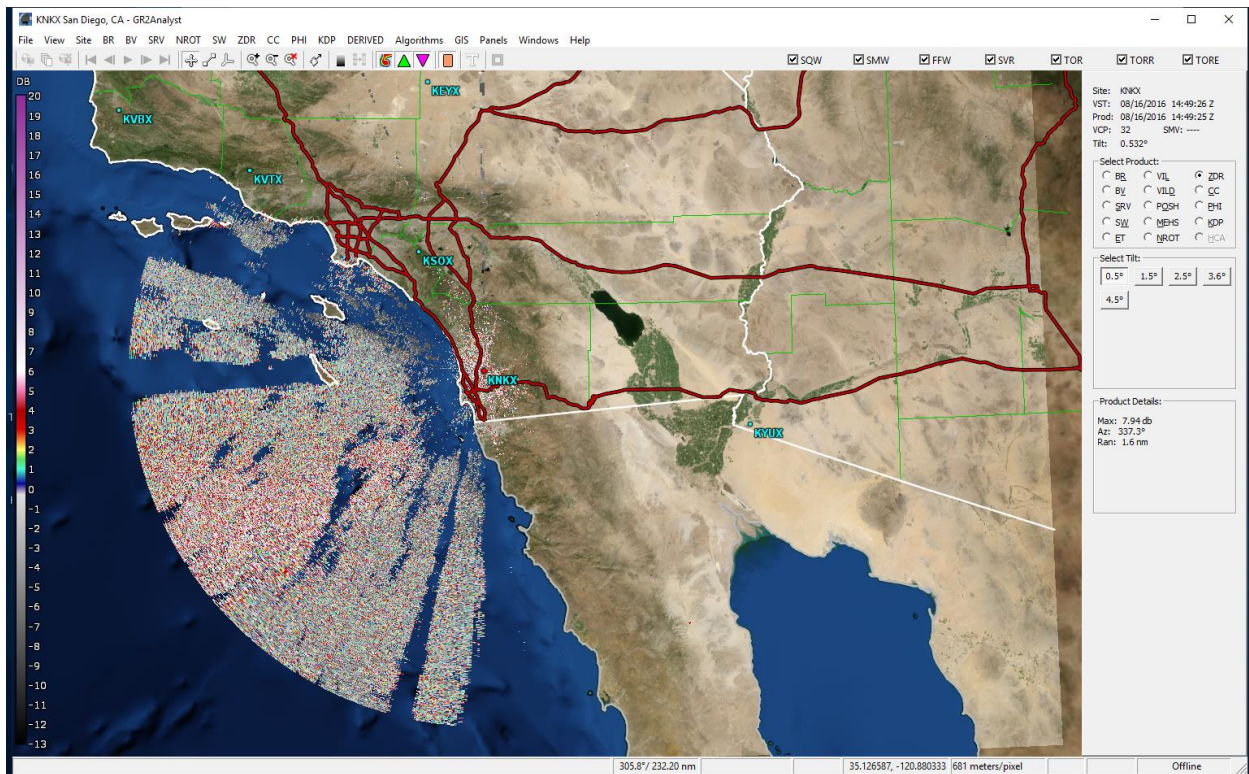


Fig. 14. ZDR field from KNKX on 16 Aug. 2016 at 1449 UTC at an elevation of 0.5°.

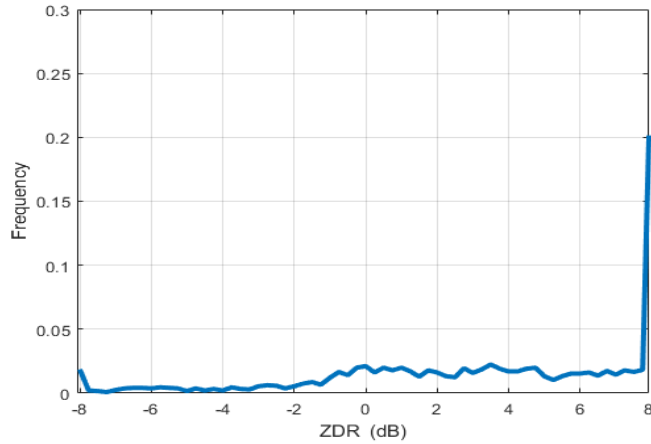


Fig. 15. Distribution of ZDR values for the case in Fig. 14. The data were obtained with the  $\pm 7.9$  dB ZDR interval.

### 3.6. Atmospheric biota

Radar echoes from insects, birds, and bats in the atmosphere exhibit large ZDR values of both signs. An example in Fig. 16 is from migrating Monarch butterflies in central Oklahoma; the images have been obtained from the level-1 data. The maximum ZDR values are larger than 18 dB (Fig. 17). Another example (Figs. 18 and 19) is from migrating birds. Some precipitation echo is in the southwest direction at ranges beyond 65 km. ZDR values within distances of 65 km lie in an interval of -12 to +15 dB. Observations with KOUN show that ZDR values from biota typically span an interval of -7 to +17 dB, but some values can be larger than 20 dB.

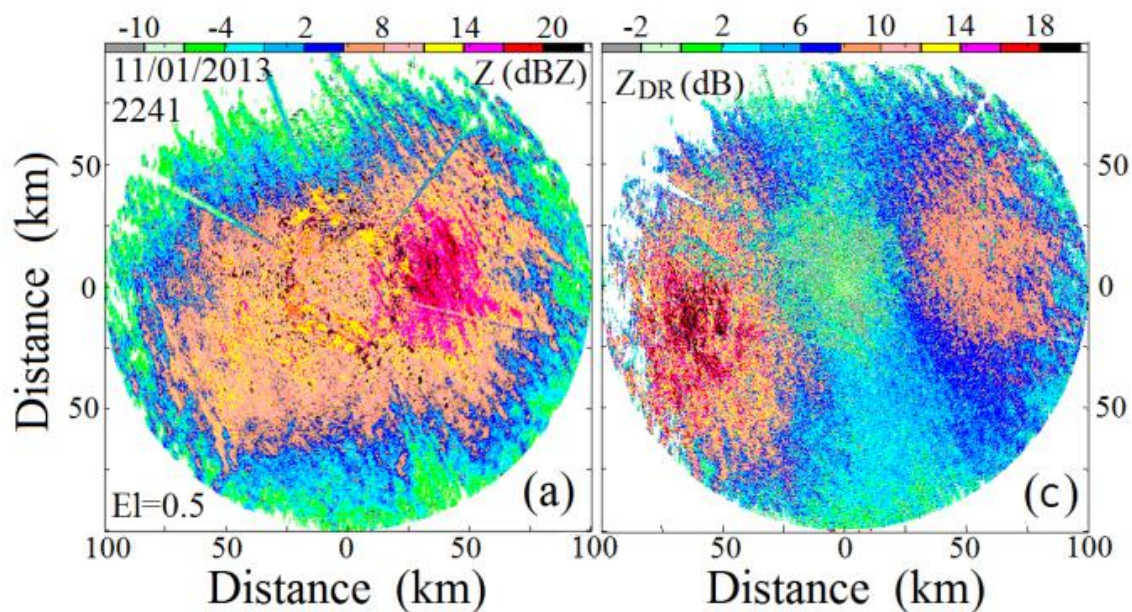


Fig. 16. Echo from insects observed with KOUN on 1 Nov. 2013 at 2241Z, the elevation is  $0.5^\circ$ .

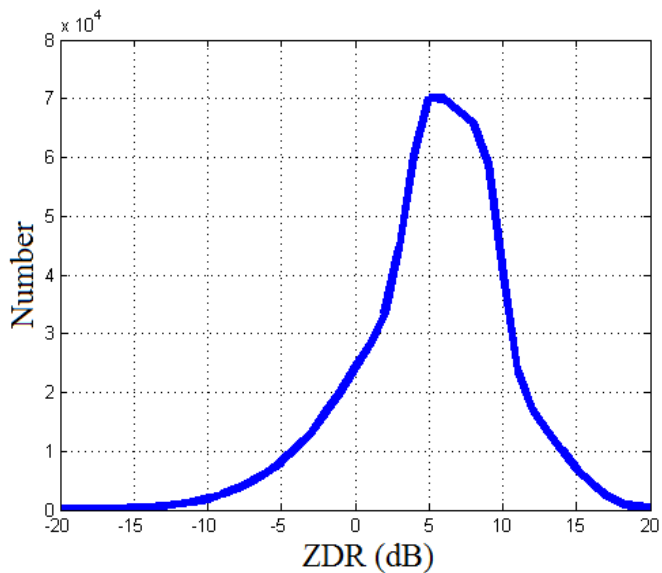


Fig. 17. Histogram of ZDR values for the case shown in Fig. 9.

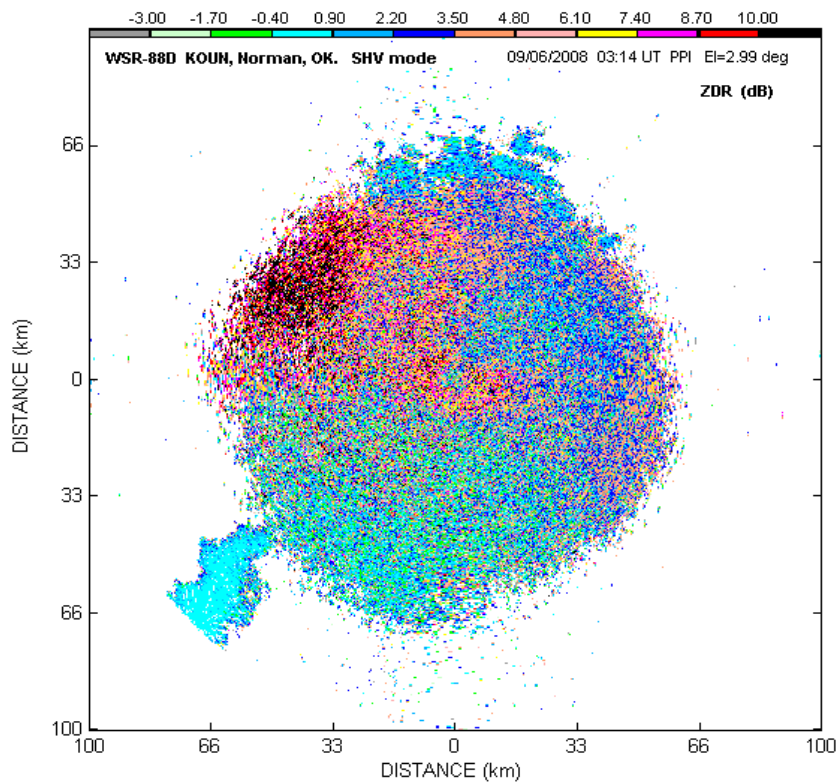


Fig. 18. ZDR field observed with KOUN on 6 Sep. 2008 at 0314Z at an elevation of  $3^\circ$ . The data have been obtained from I/Q radar signals that have no limitations in  $Z_{DR}$  values.

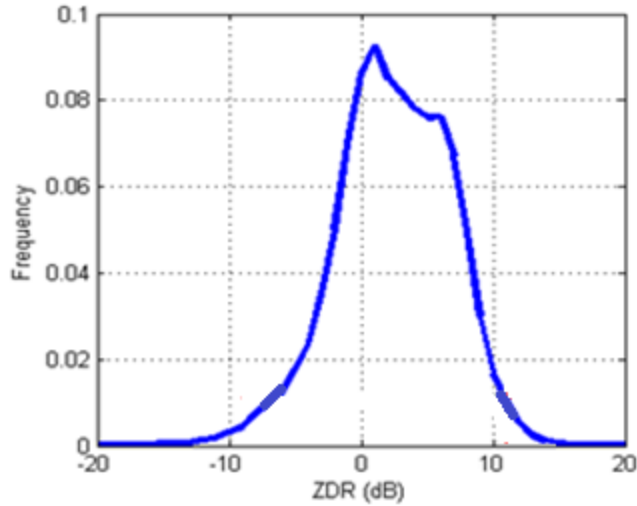


Fig. 19. Histogram of  $Z_{DR}$  values for the field in Fig. 18.

ZDR histograms show that to correctly represent ZDR values from atmospheric biota a large measurement ZDR interval is needed. A larger ZDR interval is needed to correctly separate echoes from birds and insects. A detection of birds is important for aviation for avoiding flocks of birds. Filtering out echoes from birds is useful for obtaining the wind from WSR-88D data because velocities from birds contribute to measured Doppler velocities and bias the VAD outputs.

### 3.7. Chaff

Chaff in the air was observed for the first time with a dual-polarization radar by Zrníc and Ryzhkov (2004) in central Oklahoma. A scatterplot of Z-ZDR from that work is shown in Fig. 20. The ZDR values from chaff are mostly lie in an interval from -1 to +7 dB.

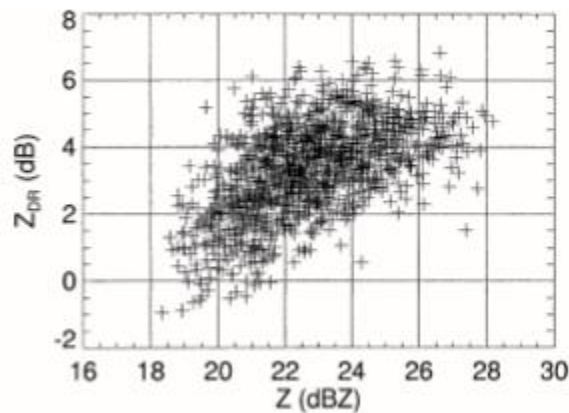


Fig. 20. Scatterplot of Z-ZDR from chaff observed with KOUN on 6 Feb. 2003 at an elevation angle of  $0.5^\circ$ . Adopted from Zrníc and Ryzhkov (2004).

Chaff is frequently observed with the WSR-88Ds in Florida and Arizona. An example of a ZDR field from chaff observed by KBYX is shown in Fig. 21 and a distribution of ZDR values from that case in a time interval 19-22 UTC is shown in Fig. 22a, and a distribution from another case is shown in Fig 22b. It can be seen from Fig. 22 that ZDR values from chaff can exceed the measurement interval  $\pm 7.9$  dB. Comparisons of ZDR values from Figs. 20 and 22 show that the median values are quite different: in Fig. 20 it is about 3 dB whereas in Fig. 22 it is about 0 dB. Fig 22 shows a large number of negative ZDR values, which are absent in Fig. 20. These features most likely point to different types/sizes of chaff being observed. Strong “horns” at values of  $\pm 8$  dB in Fig. 22 indicates many ZDR values which are out of the measurement interval  $\pm 7.9$  dB. Those data were clipped at the minimum and maximum values.

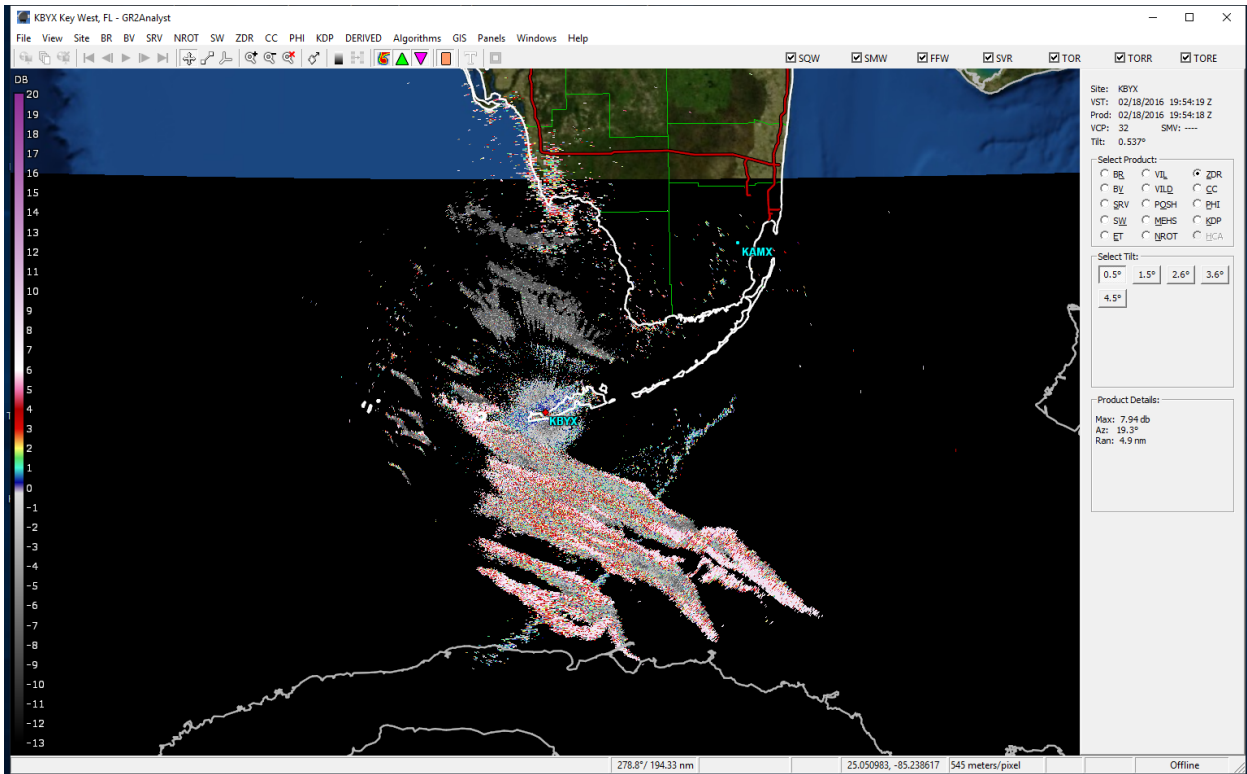


Fig. 21. Radar echo from chaff observed with KBYX on 18 Feb. 2016 at 1954 UTC at an elevation of 0.5°.

Fig. 22b presents another ZDR distribution for data collected with KBYX on 02/09/2012. Similar features can be seen in this distribution: strong spikes at the end of the measurement ZDR interval. Fig. 22 demonstrates that a larger measurement ZDR span is needed to correctly represent ZDR from chaff. A larger ZDR span will be useful for identification of chaff.

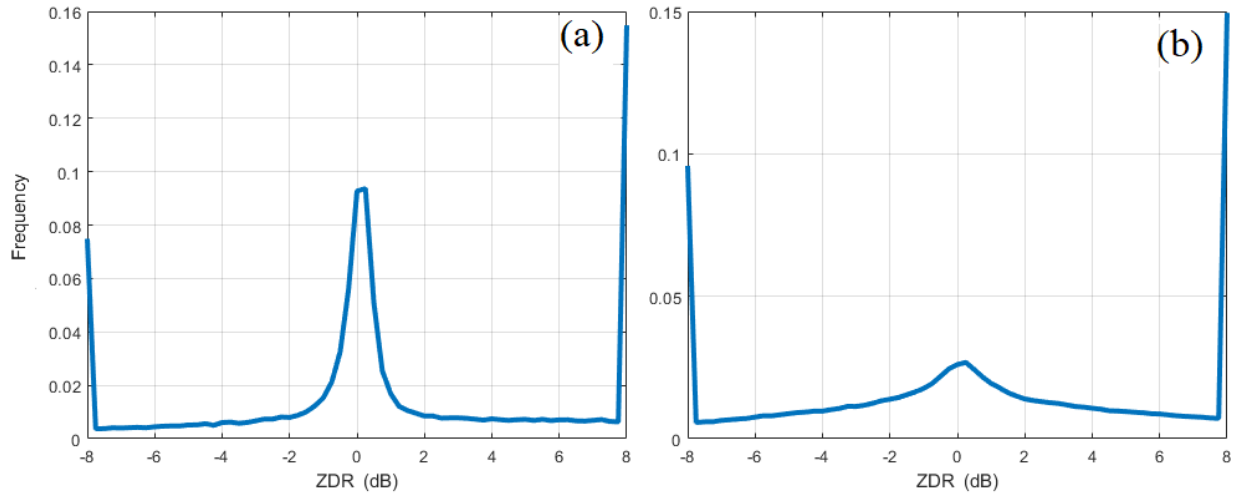


Fig. 22. ZDR distribution from chaff collected with KBYX on (a) 02/18/2016 and (b) 02/09/2012.

### 3.8. Wild fire smoke

An example of radar echoes from wild fire smoke is shown in Fig. 23 and produced from level-1 data. There were three areas of fire to the south of the radar at distances of 75 – 80 km. The fires are denoted with numbers 1, 2 and 3 in the reflectivity field. The central part of the radar echo is from insects/birds. Smoke from the fire areas stretched to the northeast for more than 100 km. A distribution of ZDR values from the smoke is shown in Fig. 24. It can be seen that ZDR values lie in an interval from about -5 dB to about 8 dB, i.e., the ZDR values barely lie within the current measurement ZDR interval of  $\pm 7.9$  dB. Different distributions in other cases could exceed the current measurement interval.

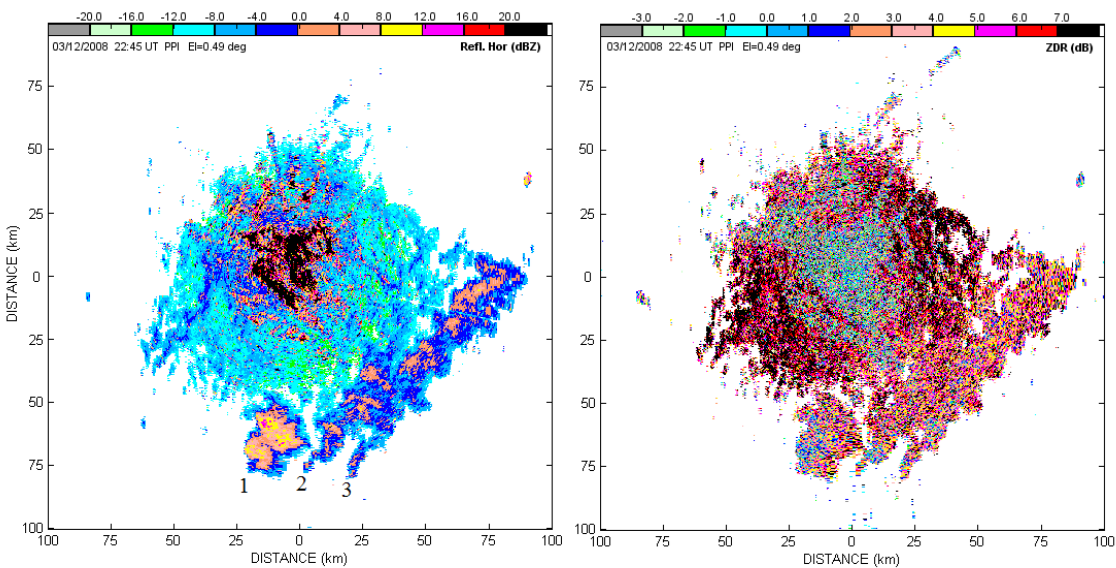


Fig. 23. Reflectivity (left) and ZDR (right) fields observed with KOUN on 12 March 2008 at 2245Z at the elevation of  $0.5^\circ$ . Numbers 1, 2, and 3 indicate the sources of smoke plumes.

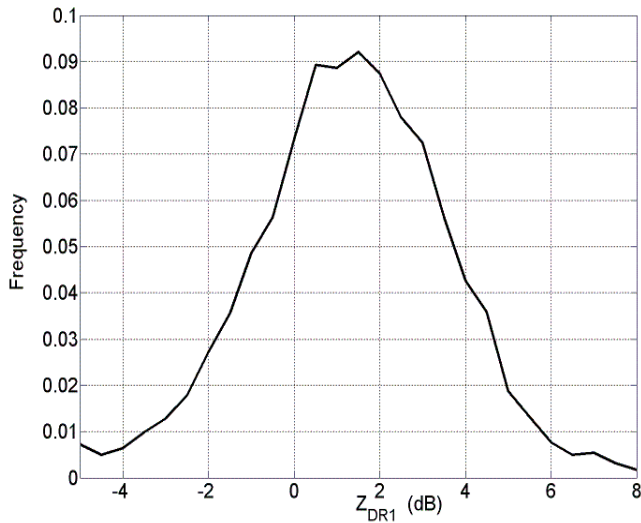


Fig. 24. Distribution of ZDR values from smoke plumes shown in Fig. 23.

### 3.9. Summary of ZDR values from various objects

The table below summarizes spans of ZDR values observed from various targets.

Target	Observed ZDR interval, dB	Subsection #
Precipitation and clouds	-4 to +15	3.1
Attenuation effects	-2 to 0	3.2
Dust storms	-2 to +12	3.3
Ground clutter	-20 to +20	3.4
Sea clutter	-15 to +15	3.5
Atmospheric biota	-12 to +17	3.6
Chaff	Less than -8 to more than +8	3.7
Wild fire smoke	-5 to +8 dB	3.8

Since the mission of the WSR-88D is primarily the identification of precipitation types, a desired ZDR interval of clouds and precipitation is from -4 to +15 dB. The ZDR value of -4 dB is obtained from a minimal ZDR observed in hail cores and possible -2dB due to of attenuation because hail cores are frequently observed inside thunderstorms, i.e., hail cores are typically observed beyond heavy rain. The measurement ZDR span of -10 to +20 dB of Build 19 will cover all possible ZDR values from clouds and precipitation.

The measurement ZDR interval of -10 to +20 dB of Build 19 will cover more than 98% of ZDR values from atmospheric biota and sea clutter and seems sufficient for recognition of those targets. ZDR values from ground exhibit a wide span, but ground clutter is strongly suppressed by ground clutter filtering and may not entirely cover the ZDR measurement interval.

#### 4. Radar observations using Build 19

WSR-88D KOUN located at Norman, OK has been running Build 19 since 20 December 2018. The RPG produces a wider ZDR span (-10 to +20 dB) that eliminates the clipping effect in weather objects. The enlarged ZDR interval uses a larger byte representation. Unfortunately, KOUN was not running in January 2019 when snow and ice clouds could be observed in central Oklahoma. KOUN could not be ran because of the government shutdown at that time. To verify the larger ZDR boundaries of the new measurement ZDR span, observations of insects and birds were carried out in 2019. An example of echo from insects in central Oklahoma is shown in Fig. 25. The central echo is from atmospheric biota. Some echo from precipitation can be seen in the north-northwest direction from the radar at distances about 220 km, where ZDR values are low. The central echo exhibits ZDR values up to 20 dB (Fig. 26). A small bump in ZDR at 20 dB indicates that some ZDR values were larger than 20 dB, but have been clipped to 20 dB.

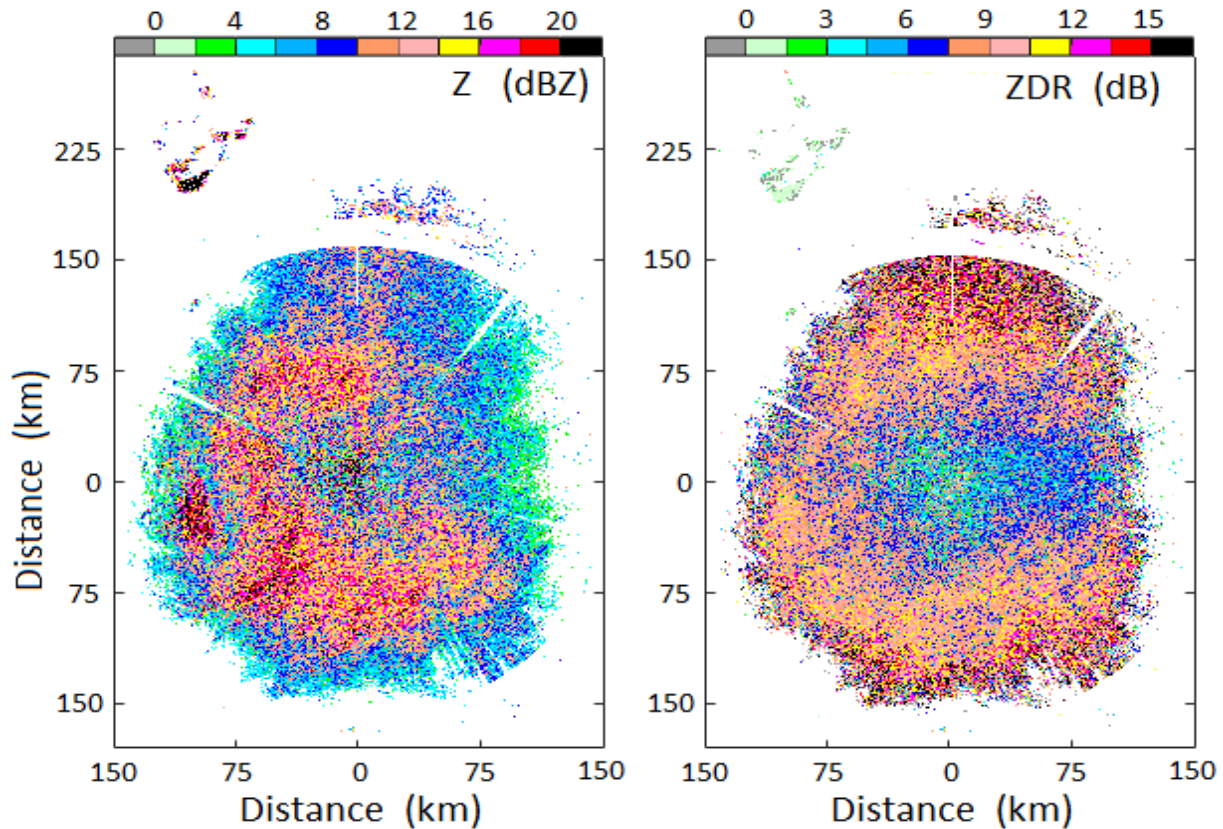


Fig. 25. Reflectivity (left panel) and ZDR (right) fields observed with KOUN July 16, 2019 at 1748 UTC at an elevation of 0.5°. KOUN is running Build 19.

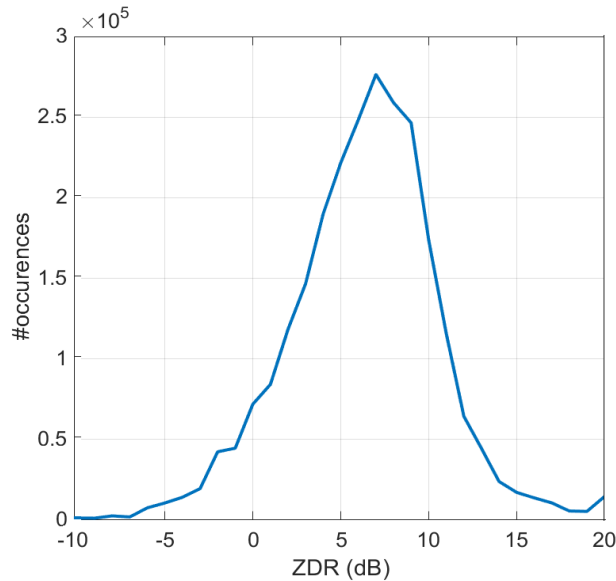


Fig. 26. ZDR distribution collected with KOUN on July 16, 2019 from 1749 till 1843 UTC at an elevation of 0.5°.

## 5. Conclusions

The current measurement ZDR interval of  $\pm 7.9$  dB does not cover all possible ZDR values from clouds and precipitation, where the maximal ZDR can reach 15 dB. The current precision of ZDR measurements of 0.06 dB is slightly larger than a required precision of 0.05 dB for the ultimate goal of the accuracy of ZDR measurements of 0.1 dB, which is desirable for measurements of light rain and snow.

A measurement ZDR span from  $-15$  to 20 dB is required for observations of various radar targets (clouds, precipitation, atmospheric biota, sea clutter, and wild fire smoke).

Build 19 features a measurement ZDR interval of  $-10$  to 20 dB, which completely covers the ZDR interval from clouds and precipitation. This interval covers about 98% of observed ZDR values from various targets, i.e., it is sufficient for correct measurements in weather and non-weather objects.

Correct ZDR measurements in non-weather objects are important for correct identification of different targets. For instance, the larger ZDR span is useful for distinguishing echoes from birds and insects in the atmosphere. Birds are a hazard for aviation. Correct identification of insect echoes free from birds will help with obtaining the atmospheric wind using the VAD technique.

## References

Dual Polarization Enhanced WSR-88D System Specifications. Document # 2810000E, 2003.

Gossard, E.E., and R.G. Strauch, 1983: *Radar Observations of Clear Air and Clouds*. Elsevier, 280 pp.

Picca, J., and A. Ryzhkov, 2012: A Dual-Wavelength Polarimetric Analysis of the 16 May 2010 Oklahoma. *Mon. Weather Rev.*, 140, 1385-1403.

RPI MOU, 2019 Report, Task 10: Impacts of the radar differential phase upon transmission on the polarimetric variables. 43 pp.

Zrnic, D.S., and A.V. Ryzhkov, 2014: Polarimetric properties of chaff. *J. Atmos. Ocean. Technol.* **21**, 1017-1024.